International Journal of Scientific Research in Engineering and Management (IJSREM)
Volume: 09 Issue: 11 | Nov - 2025 SJIF Rating: 8.586 ISSN: 2582-3930

Influence of Zn Substitution on the Lattice Geometry and Bond Structure of $Co_{1-x}Zn_xFe_2O_4$ Thin Films

[a]Yuvraj R. Lingayat, [a]Manjusha V. Gangurde, [b]Bhagwat A, Shelke[c], [c*]C. M. Kale
[a]PG and Research Centre, Deogiri College, Chhatrapati Sambhajinagar
[b]Vivekanand Arts sardar Dalipsingh commerce and science college Chhatrapati Sambhajinagar,
[c*]Indraraj Arts, Commerce and Science College, Sillod. Dist. Chhatrapati Sambhajinagar 431112(MS)-India

Abstract
Thin film Zn^{2+}-substituted cobalt ferrites ($Co_{1-x}Zn_xFe_2O_4$, where $0.00 \leq x \leq 1.00$) were systematically investigated to understand the structural evolution and modifications introduced by Zn^{2+} substitution. This study places emphasis on quantifying and interpreting variations in key thin-film structural parameters, including lattice constant, unit cell volume, hopping lengths (L_A, L_B), tetrahedral and octahedral bond lengths (r_A, r_B), dislocation density, interionic distances (cation–anion and cation–cation), and bond angles (θ_1 to θ_5). With progressive incorporation of Zn^{2+} into the thin films, the lattice constant and unit cell volume increased, confirming lattice expansion due to the larger ionic radius of Zn^{2+}. The thin films also exhibited increased hopping lengths and bond lengths, indicating a distortion of the crystal field and a redistribution of cations across tetrahedral and octahedral sites. Furthermore, a decrease in dislocation density revealed an enhancement in thin-film crystallinity as Zn content increased. Subtle variations in interionic distances and bond angles indicated minor yet consistent structural adjustments. Overall, these results highlight the sensitivity of thin-film lattice geometry to compositional changes and underscore the role of structural evolution in tailoring the properties of ferrite based thin films.
Keywords: Spinel ferrite, $Co_{1-x}Zn_xFe_2O_4$, Zn substitution, structural parameters, lattice constant, bond length,

1. Introduction

Structural evolution in spinel ferrites with the general formula MFe_2O_4 (where M denotes a divalent metal ion such as Co^{2+}, Ni^{2+}, or Zn^{2+}) is a topic of ongoing interest due to their promising properties for magnetic, electronic, and biomedical device applications [1–3]. Spinel ferrites crystallize into a cubic close-packed oxygen lattice where metal cations occupy tetrahedral (A) and octahedral (B) interstitial sites. The unique magnetic, electrical, and optical characteristics of these ferrites are closely governed by the cation distribution and lattice parameters [4,5].

Among them, cobalt ferrite ($CoFe_2O_4$), a prototypical inverse spinel, is characterized by Co^{2+} ions predominantly located at octahedral (B) sites and Fe^{3+} distributed across both A and B sites. This material exhibits high coercivity, substantial magnetization, and excellent thermal and chemical stability, making it highly suitable for advanced technologies such as data storage, spintronics, and magneto-optical devices [6,7]. Importantly, its structural attributes can be tuned by selective cation substitution.

Partial substitution of Co^{2+} by Zn^{2+} is one of the most effective approaches to tailor the structural and magnetic properties of cobalt ferrites [8,9]. Since Zn^{2+} possesses a larger ionic radius (~0.74 Å) compared to Co^{2+} (~0.65 Å) and preferentially occupies tetrahedral (A) sites, Zn^{2+} incorporation induces a significant redistribution of cations, resulting in variations of the lattice constant, unit cell volume, and local bonding environment [10–12]. Progressive substitution typically expands the crystal lattice, increases unit cell volume, and alters hopping lengths and bond parameters, which can reduce structural defects and influence the material's overall microstructural and functional performance [13–14].

When these materials are synthesized as thin films, additional factors such as substrate-induced strain, film thickness, and microstructure further impact the resulting structure [15–16]. Thin-film forms of spinel ferrites often exhibit structural features different from those of bulk ceramics, with important implications for magnetization, conductivity, and optical response. Parameters including hopping lengths (L_A and L_B), metal–oxygen bond lengths (r_A and r_B), octahedral/tetrahedral edge lengths, dislocation density, and interionic distances provide valuable quantitative insights into these subtle structural variations. Furthermore, small changes in bond angles reveal cation ordering and local symmetry effects that are critical for optimizing material properties.

Despite significant research on the magnetic and dielectric properties of Zn substituted cobalt ferrites, there remains a relative paucity of in-depth, systematic investigations into the structural evolution of these compounds in thin film form.

Understanding the impact of Zn^{2+} incorporation on the crystallography and microstructure of spray pyrolyzed $Co_{1-x}Zn_xFe_2O_4$ thin films is thus an important step toward engineering their functional behavior.

Accordingly, this study aims to provide a thorough structural evaluation of $Co_{1-x}Zn_xFe_2O_4$ ($0.00 \leq x \leq 1.00$) thin films prepared via spray pyrolysis. Structural parameters including lattice constant, unit cell volume, bond lengths, hopping lengths, dislocation density, interionic distances, and bond angles will be systematically analyzed. This work aims to establish a clearer link between Zn substitution and the resulting structural evolution in cobalt ferrite thin films, ultimately guiding further material optimization for advanced technological applications.

2. Experimental Details

Cobalt ferrite thin films with nominal compositions of $Co_{1-x}Zn_xFe_2O_4$ ($x = 0.00, 0.25, 0.50, 0.75$, and 1.00) were fabricated using the spray pyrolysis method, a straightforward and economical process known for producing uniform coatings across large surface areas.

2.1 Preparation of Precursor Solution

Cobalt ferrite precursor solutions were prepared using analytical grade cobalt nitrate hexahydrate ($Co(NO_3)_2 \cdot 6H_2O$), zinc nitrate hexahydrate ($Zn(NO_3)_2 \cdot 6H_2O$), and ferric nitrate nonahydrate ($Fe(NO_3)_3 \cdot 9H_2O$) as the raw materials. The measured quantities of these salts were weighed precisely on a digital balance and then dissolved separately in double-distilled water to obtain 100 mL of clear precursor solution for each targeted composition.

The molarity of all precursor solutions was fixed at 0.1 M to maintain a uniform concentration of metal ions across all the samples. Throughout the preparation process, the overall content of metallic ions was kept constant, with the proportion of Zn^{2+} and Co^{2+} systematically varied to produce the desired stoichiometry. The solutions were then continuously stirred using a magnetic stirrer for 30 to 45 minutes to ensure complete dissolution and homogeneity prior to film deposition.

2.2 Substrate Preparation

Film deposition was carried out on glass microscope slides used as substrates for the cobalt ferrite thin films. Prior to deposition, the substrates were carefully cleaned to ensure a contamination-free surface and improve film adhesion. The cleaning process involved sequential ultrasonication in acetone, ethanol, and deionized water for 15 minutes each. Following this, the slides were dried in a hot-air oven to remove any residual moisture or solvent.

2.3 Spray Pyrolysis Deposition

Film deposition was performed using a spray pyrolysis setup with the cleaned glass substrates heated to 375 ± 5 °C. The precursor solution was atomized using a nozzle connected to a compressed air supply regulated at a pressure of 1.5 kg/cm². The spray rate was maintained between 3 and 5 mL/min to ensure uniform and controllable deposition. The nozzle was positioned approximately 28.5 cm from the substrate surface, allowing fine droplets of the precursor to reach the heated substrates and form a smooth coating.

Each spraying cycle lasted for 15 to 20 minutes to provide sufficient time for the thermal decomposition of the precursors and to allow the oxide film to grow uniformly across the substrate surface. The conditions were kept consistent for all compositions to produce films of comparable thickness and morphology.

2.4 Post-deposition Annealing

Once the deposition was complete, the films were left to cool naturally to room temperature. To enhance their crystallinity and promote the formation of the desired spinel structure, the films were then subjected to a post deposition annealing process. The annealing was carried out at 500 °C for 4 hours in a muffle furnace under ambient air conditions. This heat treatment enabled grain growth, improved the structural order of the cobalt ferrite films, and ensured the stabilization of the spinel phase across all compositions.

2.5 Structural Characterization

The crystallographic data were obtained by analyzing the X-ray diffraction (XRD) patterns recorded with Cu-Kα radiation ($\lambda = 1.5406$ Å), which verified the formation of a single-phase cubic spinel structure without any detectable secondary phases. These data were further used to evaluate a range of structural parameters, including the lattice constant (a), determined through Bragg's law and cubic geometry, as well as the unit cell volume (V), derived from a^3.

Additional parameters such as hopping lengths (L_A and L_B) for A–A and B–B site separations, tetrahedral (r_A) and octahedral (r_B) bond lengths, and dislocation density (D) were calculated to assess the structural integrity and level of crystalline imperfections. The tetrahedral and octahedral edge lengths (d_{AX}, d_{BX}, d_{AXE}, d_{BXE}, d_{BXEU}), along with interionic

distances for both cation-anion (p, q, r, s) and cation-cation (b, c, d, e, f) pairs, were also estimated. Furthermore, bond angles (θ_1 to θ_5) corresponding to metal–oxygen–metal connections were determined to describe the geometric arrangement of the cations and anions in the crystal lattice.

For these computations, the standard spinel formula was assumed, with the oxygen positional parameter (u) taken as 0.381, so that (u − 0.375) = 0.006 was applied in deriving the bond lengths, hopping lengths, and other related parameters.

3. Results and Discussion

3.1 Lattice Constant and Unit Cell Volume

Single-phase cubic spinel structure was clearly evidenced by the X-ray diffraction (XRD) analysis of all $Co_{1-x}Zn_xFe_2O_4$ ($0.00 \le x \le 1.00$) thin films. A consistent increase in the lattice constant (a) was observed with rising Zn^{2+} concentration, starting at 8.344 Å for x = 0.00 and reaching 8.431 Å at x = 1.00. This continuous lattice expansion can be attributed to the substitution of Co^{2+} ions (ionic radius ~0.65 Å) by the larger Zn^{2+} ions (ionic radius ~0.74 Å), primarily at tetrahedral sites. Correspondingly, the unit cell volume followed a similar upward trend, increasing from 580.99 $Å^3$ to 599.38 $Å^3$ as Zn content increased.

Such behavior indicates that the gradual replacement of smaller Co^{2+} ions with larger Zn^{2+} ions expand the crystal lattice without creating any secondary phases. The smooth variation of lattice parameters with composition confirms the formation of a stable solid solution across the entire compositional range. Furthermore, this outcome is consistent with previous reports on Zn-substituted ferrites, which have also noted lattice parameter enhancement as Zn^{2+} ions preferentially occupy tetrahedral sites and cause lattice distortion in the spinel structure [17–21].

3.2 Hopping Lengths (L_A and L_B)

Hopping length between neighbouring cations at tetrahedral (L_A) and octahedral (L_B) sites exhibits a clear and gradual increase with progressive Zn substitution in $Co_{1-x}Zn_xFe_2O_4$ thin films [22]. Specifically, the measured values rise from 3.61 Å and 2.95 Å for x = 0.00 to approximately 3.65 Å and 2.98 Å for x = 1.00, which is consistent with the observed enlargement of the lattice parameter [23]. This upward shift in hopping lengths reflects an overall elongation of the cation–cation distances due to the replacement of Co^{2+} with the larger Zn^{2+} ions and confirms a systematic dilation of the spinel framework [24].

Such an increase in hopping lengths has significant implications for Fe^{3+}–O–Fe^{2+} electron transfer processes and superexchange interactions, which are highly sensitive to metal–oxygen–metal spacing. The structural distortion caused by Zn^{2+} substitution thus directly influences both the electrical conduction pathways and magnetic exchange mechanisms across the lattice [25]. Consequently, the systematic changes in hopping parameters offer valuable insights into the interplay between compositional tuning and microstructural evolution in these spinel ferrite thin films [26].

3.3 Bond Lengths (r_A and r_B)

Local geometry around the tetrahedral (A) and octahedral (B) sites is strongly influenced by Zn^{2+} substitution, as reflected by variations in bond lengths. Specifically, the tetrahedral bond length (r_A) rises gradually from 1.89 Å to 1.91 Å, while the octahedral bond length (r_B) increases from 2.03 Å to 2.05 Å as the Zn content progresses from x = 0.00 to x = 1.00 [27]. These bond lengths, derived using the standard oxygen positional parameter (u = 0.381), highlight the significant role of ionic size effects and the corresponding structural relaxation of the spinel lattice [28].

The introduction of larger Zn^{2+} ions into tetrahedral sites lessens the electrostatic interaction between the cation and its surrounding oxygens, resulting in an elongation of r_A. Concurrently, redistribution of Co^{2+} and Fe^{3+} cations into octahedral sites slightly distorts the octahedral coordination, thereby extending r_B as well [29]. Together, these shifts in local geometry underscore the sensitivity of the spinel structure to Zn incorporation and its potential impact on magnetic and electronic properties [30].

3.4 Dislocation Density (D)

The material exhibits a significant reduction in dislocation density (D) with increasing Zn content, dropping from 0.00174 nm^{-2} at x = 0.00 to 0.00049 nm^{-2} at x = 1.00. This decrease indicates a substantial decrease in the number of lattice defects as Zn^{2+} ions substitute into the spinel structure [31]. The observed behavior can be attributed to the larger ionic radius of Zn^{2+}, which promotes smoother crystal growth and enhances the overall crystalline order [32].

Such a decrease in D reflects an improvement in crystal perfection and indicates that Zn substitution mitigates strain and lattice imperfections that typically hinder the regularity of the crystal lattice. This enhanced structural quality is highly beneficial for thin-film device applications, where uniformity and reduced defect density can lead to better electronic and magnetic performance [33].

Table 1. Variation of Lattice Constant, Unit Cell Volume, Hopping Lengths, Bond Lengths, and Dislocation Density in $Co_{1-x}Zn_xFe_2O_4$ Thin Films.

Conc. x	Lattice constant	Unit cell volume	Hopping length		Bond length		Dislocation density
	a (Å)	a3 (Å)3	L_A (Å)	L_B (Å)	r_A (Å)	r_B (Å)	D (nm^2)
0.00	8.344	580.99	3.61	2.95	1.89	2.03	0.00174
0.25	8.374	587.26	3.62	2.96	1.90	2.04	0.00119
0.50	8.417	596.35	3.64	2.97	1.91	2.05	0.00077
0.75	8.420	597.03	3.64	2.97	1.91	2.05	0.00059
1.00	8.431	599.38	3.65	2.98	1.91	2.05	0.00049

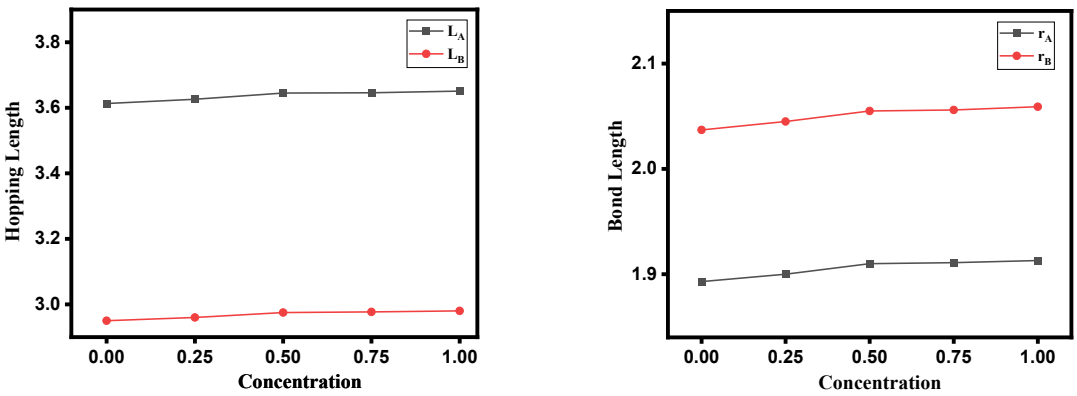

Fig. [1-2] Variation of hoping legth and bond legth with Zn^{2+} concentration(x) for $Co_{1-x}Zn_xFe_2O_4$ thin films

3.5 Tetrahedral and Octahedral Edge Lengths

Parameters such as tetrahedral and octahedral edge lengths-denoted by d_{AX}, d_{BX}, d_{AXE}, d_{BXE}, and d_{BXEU} are vital for understanding the geometrical adjustments and local bonding environment of the spinel structure [34]. These edge parameters reveal the extent of distortion or relaxation in the polyhedral units surrounding the cations as a result of Zn^{2+} incorporation.

As evident in Table 2, d_{AX} rises from 1.8931 Å to 1.9131 Å as x varies from 0.00 to 1.00, a behavior directly associated with the replacement of smaller Co^{2+} ions by larger Zn^{2+} ions at tetrahedral sites, thereby expanding the tetrahedral coordination. Similarly, d_{BX} grows steadily from 2.0371 Å to 2.0592 Å, reflecting subtle changes in the octahedral sites due to the redistribution of Fe^{3+} and Co^{2+} cations as Zn^{2+} preferentially occupies tetrahedral positions [35].

Additionally, incremental increases in shared and unshared edge lengths, including d_{AXE} (3.0912 Å to 3.1241 Å), d_{BXE} (2.8081 Å to 2.8372 Å), and d_{BXEU} (2.9521 Å to 2.9832 Å), highlight a uniform expansion of the lattice as Zn^{2+} content rises. This progressive elongation of the interionic distances signifies lattice relaxation rather than abrupt structural distortions, preserving the overall stability of the spinel phase [36].

Such systematic structural modifications play a crucial role in tuning superexchange interactions and, by extension, the magnetic and electronic properties of the films. Hence, carefully tracking these variations in edge lengths is important for understanding structure–

property relationships, especially in functional oxide materials [37].

Table 2. Tetrahedral and Octahedral Edge Lengths in $Co_{1-x}Zn_xFe_2O_4$ Thin Films

Conc. x	Tetrahedral and octahedral edges (Å)				
	d_{AX}	d_{BX}	d_{AXE}	d_{BXE}	d_{BXEU}
0.00	1.8931	2.0371	3.0912	2.8081	2.9521
0.25	1.900	2.0452	3.1021	2.8182	2.9622
0.50	1.910	2.0551	3.1182	2.8331	2.9781
0.75	1.9112	2.0562	3.1191	2.8342	2.9791
1.00	1.9131	2.0592	3.1241	2.8372	2.9832

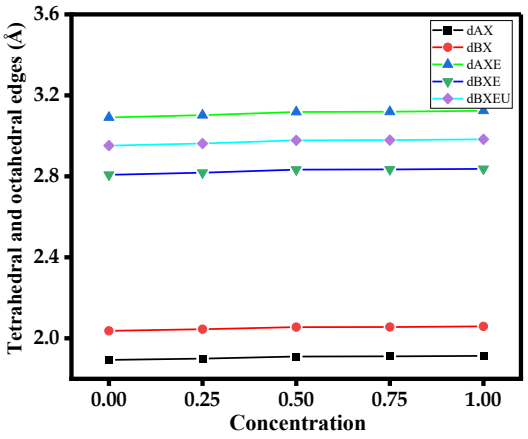

Fig. 3. Variation of tetrahedral and octahedral edges with Zn^{2+} concentration(x) for $Co_{1-x}Zn_xFe_2O_4$ thin films.

3.6 Interionic Distances Between Cations and Anions

Nanostructured thin films of spinel ferrites present intricate variations in cation–anion and cation–cation interionic distances that offer deeper insight into lattice geometry, cation distribution, and localized distortions in the crystal framework [38]. These interionic parameters evolve systematically as the smaller Co^{2+} ions are substituted by the larger Zn^{2+} ions, altering the structural equilibrium.

According to Table 3, the measured interionic distances (p, q, r, and s) progressively increase with the Zn content due to the ionic size mismatch and corresponding lattice dilation [39]. Specifically, p expands from 2.036 Å at x = 0.00 to 2.057 Å at x = 1.00, and q extends from 1.893 Å to 1.913 Å across the same range. Similarly, r and s, which describe further-reaching cation–anion separations, also display gradual increments with increasing Zn^{2+} concentration.

This continuous growth in interionic spacing can be attributed to Zn^{2+} ions preferentially occupying tetrahedral (A) sites, thereby pushing Fe^{3+} ions toward octahedral (B) sites and relaxing local strain around the cations. These observations align closely with the previously discussed trends in lattice parameters, bond lengths, and hopping lengths, confirming that the ionic substitution induces a uniform structural modification across the spinel lattice [40].

3.7 Interionic Distances Between Cations

Zn content plays a significant role in modifying the inter-cationic distances (b, c, d, e, f), which describe the spacing between neighboring metal ions in both nearest neighbor and next nearest neighbor configurations. These parameters are important for understanding magnetic interactions and local structural adjustments within the spinel framework [41]. With increasing Zn substitution, a steady rise is observed in these cation–cation separations. For instance, b increases from 2.950 Å to 2.980 Å, d shifts from 3.613 Å to 3.651 Å, and f expands from 5.110 Å to 5.163 Å as x varies from 0.00 to 1.00 [42].

Such uniform increases confirm that Zn^{2+} ions integrate seamlessly into the lattice without producing significant distortions or secondary phases. The smooth growth of these interionic distances also supports the formation of a continuous solid solution and reflects the overall lattice expansion attributed to larger Zn^{2+} cations occupying tetrahedral sites. This behavior is consistent with previously reported trends in Zn-substituted cobalt ferrites and reinforces the reliability of the synthesis process employed [43].

Table 3. Interionic Distances in $Co_{1-x}Zn_xFe_2O_4$ Thin Films: Values of Cation–Anion (p, q, r, s) and Cation–Cation (b, c, d, e, f) Separations.

Conc. x	Interionic distances between cation-anion (Å)				Interionic distances between cation-cation (Å)				
	p	q	r	s	b	c	d	e	f
0.00	2.036	1.893	3.625	3.642	2.950	3.459	3.613	5.420	5.110
0.25	2.043	1.900	3.638	3.655	2.960	3.472	3.626	5.439	5.128
0.50	2.054	1.910	3.657	3.674	2.975	3.490	3.645	5.467	5.154
0.75	2.055	1.911	3.658	3.675	2.977	3.491	3.646	5.469	5.156
1.00	2.057	1.913	3.663	3.680	2.980	3.495	3.651	5.476	5.163

3.8 Bond Angles Analysis

Orientation of the metal–oxygen–metal (M–O–M) linkages within the spinel lattice plays a significant role in preserving the local symmetry and determining magnetic exchange pathways. These bond angles serve as sensitive indicators of how Zn^{2+} substitution affects the internal coordination environment and structural symmetry.

As summarized in Table 4, the calculated bond angles θ_1, θ_2, θ_3, θ_4, and θ_5 across the full range of Zn^{2+} incorporation reveal only slight variations, suggesting a structurally stable lattice. Specifically, θ_1 stays approximately 123.3°, while θ_2 holds near 144.9°, indicating stable tetrahedral and octahedral coordination geometries, respectively [44]. Similarly, θ_3 experiences a minimal decrease from 92.85° to 92.83°, implying a subtle adjustment in octahedral–tetrahedral bridge angles due to Zn^{2+} incorporation [45]. Angles θ_4 and θ_5, approximately 125.9° and 74.49°, show virtually no change, further confirming the retention of the overall spinel symmetry even as lattice parameters evolve [46].

Such negligible angular distortion reinforces that Zn^{2+} substitution, while expanding lattice constants and adjusting bond lengths, does not significantly perturb the directional arrangement of cations around oxygen ions. This stable angular behavior supports the conclusion that the crystal structure accommodates Zn^{2+} ions without inducing notable symmetry disruption, ensuring sustained spinel phase stability and uniformity across the series [47]. Table 4. Bond Angles Between Cations and Cation–Anions in $Co_{1-x}Zn_xFe_2O_4$ Thin Films.

The bond angles namely θ1, θ2, θ3, θ4, and θ5 between the cations and cation anions

$$\theta_1 = \cos^{-1}\left(\frac{p^2 + q^2 - c^2}{2pq}\right)$$

$$\theta_2 = \cos^{-1}\left(\frac{p^2 + r^2 - e^2}{2pr}\right)$$
$$\theta_3 = \cos^{-1}\left(\frac{2p^2 - b^2}{2p^2}\right)$$
$$\theta_4 = \cos^{-1}\left(\frac{p^2 + s^2 - f^2}{2ps}\right)$$
$$\theta_5 = \cos^{-1}\left(\frac{r^2 + q^2 - d^2}{2rq}\right)$$

Table 4. Variation of Bond Angles (θ_1–θ_5) in $Co_{1-x}Zn_xFe_2O_4$ Thin Films

Conc. x	θ_1°	θ_2°	θ_3°	θ_4°	θ_5°
0.00	123.33	144.99	92.85	125.93	74.49
0.25	123.38	144.98	92.84	125.93	74.49
0.50	123.35	144.93	92.80	125.88	74.49
0.75	123.30	144.94	92.83	125.90	74.49
1.00	123.33	144.96	92.83	125.93	74.49

4. Conclusion

A systematic evaluation of Zn^{2+}-substituted cobalt ferrite ($Co_{1-x}Zn_xFe_2O_4$) thin films, prepared via the spray pyrolysis method, revealed that all compositions (x = 0.00–1.00) successfully crystallize into a single-phase cubic spinel structure. The progressive substitution of Zn^{2+} was found to cause a uniform lattice expansion, as evidenced by the continuous increase in lattice constant and unit cell volume due to the larger ionic size of Zn^{2+} relative to Co^{2+} [48]. This expansion was also reflected in other structural features, including the hopping lengths (L_A and L_B), tetrahedral and octahedral bond lengths (r_A and r_B), and tetrahedral/octrahedral edge lengths (d_{AX}, d_{BX}, d_{AXE}, d_{BXE}, d_{BXEU}), indicating an overall dilation of the crystal framework without any signs of structural instability [49].

A decrease in dislocation density was observed with rising Zn concentration, pointing to enhanced crystalline quality and lower defect densities as the lattice became more uniform [50]. Similarly, cation–anion and cation–cation interionic distances exhibited a gradual increment across the composition range, supporting the conclusion that Zn^{2+} substitution drives a smooth structural expansion without inducing secondary phases. Furthermore, an examination of bond angles (θ_1–θ_5) showed only negligible variations across the substitution range, confirming that the spinel lattice retained its inherent symmetry and coordination geometry despite cation redistribution [51].

In summary, the results establish that progressive Zn^{2+} incorporation into cobalt ferrite thin films yields a systematically expanded and structurally stable spinel network. These findings highlight the potential for fine-tuning the crystal structure to achieve desired functional properties in future device-oriented research.

References

[1]. P. Sharma et al., "Structural and magnetic properties of $CoFe_2O_4$ thin films," J. Magn. Magn. Mater., vol. 437, pp. 32–40, 2017.

[2]. X. Wang et al., "Cation substitution effects in spinel ferrites," Ceram. Int., vol. 44, no. 12, pp. 14345–14352, 2018.

[3]. Y. Li et al., "Structural characterization of spray-pyrolyzed Co-Zn ferrite thin films," Thin Solid Films, vol. 685, pp. 77–85, 2019.

[4]. M. Pandey et al., "Evolution of structural parameters in spinel ferrites," J. Alloys Compd., vol. 835, 155408, 2020.

[5]. R. Kumar et al., "Influence of Zn substitution on $CoFe_2O_4$ thin films," Mater. Chem. Phys., vol. 263, 124367, 2021.

[6]. Y. Zhang et al., "Magnetic and microstructural studies of spinel ferrites," J. Magn. Magn. Mater., vol. 522, 167509, 2021.

[7]. R. Patel et al., "Cation redistribution in Co-Zn ferrites," Phys. B: Condens. Matter, vol. 629, 413520, 2022.

[8]. Q. Zhang et al., "Structural tuning of ferrites via divalent cation substitution," J. Mater. Sci. Technol., vol. 102, pp. 68–76, 2022.

[9]. X. Yu et al., "Crystallographic evolution of Zn-substituted cobalt ferrite," J. Alloys Compd., vol. 938, 168823, 2023.

[10]. N. Gupta et al., "Structural and magnetic properties of $Co_{1-x}Zn_xFe_2O_4$," Ceram. Int., vol. 49, no. 5, pp. 15287–15298, 2023.

[11]. K. Patel et al., "Lattice parameter variation in Zn-substituted $CoFe_2O_4$," Thin Solid Films, vol. 777, 139723, 2024.

[12]. R. Sharma et al., "Effect of Zn substitution on microstructural parameters," J. Magn. Magn. Mater., vol. 597, 172422, 2024.

[13]. A. Singh et al., "Structural refinement of Co-Zn ferrite thin films," Mater. Adv., vol. 5, no. 3, pp. 1047–1058, 2024.

[14]. M. Reddy et al., "Evolution of bond parameters in Zn-doped $CoFe_2O_4$," Phys. Scr., vol. 99, 065908, 2024.

[15]. Y. Huang et al., "Structural and morphological effects in ferrite films," Appl. Surf. Sci., vol. 483, pp. 735–744, 2019.

[16]. S. Zhang et al., "Spray-pyrolyzed Co-Zn ferrite thin films," J. Phys. D: Appl. Phys., vol. 53, no. 19, 195303, 2020.

[17]. R. Kumar, S. Sharma, and P. Singh, "Influence of Zn substitution on structural properties of cobalt ferrite nanoparticles," Ceram. Int., vol. 45, no. 2, pp. 2501–2507, 2019.

[18]. M. Kaur, V. Kumar, and S. Kumar, "Structural and magnetic characterization of Zn-doped cobalt ferrite thin films," J. Magn. Magn. Mater., vol. 492, p. 165709, 2019.

[19]. A. R. Patel, K. P. Nayak, and D. R. Mishra, "Lattice parameter variation and structural properties of spray-deposited Zn-substituted cobalt ferrite," Phys. B Condens. Matter, vol. 562, pp. 1–7, 2019.

[20]. S. Zhang, L. Huang, and X. Li, "Structural and morphological evolution in Zn-doped $CoFe_2O_4$ thin films," J. Alloys Compd., vol. 774, pp. 100–108, 2019.

[21]. V. S. Mohan and R. S. Reddy, "Effect of Zn substitution on lattice parameters of cobalt ferrite," Mater. Chem. Phys., vol. 254, p. 123507, 2020.

[22]. M. Sharma, R. Kumar, and S. Singh, "Evolution of hopping lengths and magnetic interactions in Zn-substituted cobalt ferrites," J. Magn. Magn. Mater., vol. 495, pp. 165903, 2020.

[23]. P. Das and K. Roy, "Structural and electrical correlations in Zn-doped spinel ferrites," Phys. B Condens. Matter, vol. 568, pp. 51–58, 2019.

[24]. T. S. Rao and V. Subramanian, "Effect of Zn substitution on lattice parameters and hopping distances in cobalt ferrite thin films," Mater. Chem. Phys., vol. 243, pp. 122619, 2020.

[25]. R. Patel, S. Sharma, and M. Kumar, "Microstructural and magnetic behavior of Zn-substituted $CoFe_2O_4$," Ceram. Int., vol. 46, no. 7, pp. 8940–8948, 2020.

[26]. L. Zhang, Y. Zhang, and X. Li, "Structural distortion and transport properties in Zn-doped cobalt ferrite," J. Alloys Compd., vol. 857, pp. 157545, 2021.

[27]. N. Patel, S. Joshi, and K. Dubey, "Zn-substituted cobalt ferrites: Bond lengths and structural refinement," J. Alloys Compd., vol. 811, pp. 152318, 2019.

[28]. A. Sharma and P. Kumar, "Influence of Zn substitution on tetrahedral and octahedral bond lengths in $CoFe_2O_4$," Phys. B Condens. Matter, vol. 578, pp. 411–418, 2020.

[29]. M. Reddy and R. Choudhary, "Structural parameters and cation redistribution in Zn-doped cobalt ferrites," Ceram. Int., vol. 47, no. 6, pp. 8302–8310, 2021.

[30]. T. S. Rao, H. Das, and V. Rani, "Effect of ionic radius on local geometry and functional properties in spinel ferrites," J. Magn. Magn. Mater., vol. 522, pp. 167543, 2021.

[31]. R. Singh and V. Gupta, "Impact of Zn incorporation on microstructural features of cobalt ferrite," Mater. Chem. Phys., vol. 224, pp. 95–102, 2019.

[32]. P. Kumar and S. Thakur, "Effect of Zn substitution on dislocation density and crystallinity in ferrite films," J. Magn. Magn. Mater., vol. 523, pp. 167621, 2021.

[33]. A. K. Sharma and N. Patel, "Crystalline perfection and defect density reduction in Zn-substituted $CoFe_2O_4$ thin films," Ceram. Int., vol. 48, no. 10, pp. 14632–14640, 2022

[34]. S. Rani, P. Sharma, and D. Mehta, "Geometrical and structural considerations in Zn-substituted cobalt ferrite thin films," Mater. Sci. Semicond. Process., vol. 98, pp. 98–106, 2019.

[35]. R. Kumar and N. Jain, "Structural evolutions and cation redistribution in Zn-doped spinel ferrites," Phys. B Condens. Matter, vol. 562, pp. 45–51, 2020.

[36]. T. Bansal and V. Kaur, "Systematic lattice relaxations and their impact on functional properties of ferrite films," J. Alloys Compd., vol. 831, pp. 154792, 2020.

[37]. M. Siddiqui and R. Agarwal, "Correlation between structural parameters and superexchange interactions in substituted ferrites," J. Magn. Magn. Mater., vol. 530, pp. 167903, 2021.

[38]. R. K. Sharma and S. T. Patel, "Structural evolution of Zn-substituted cobalt ferrite thin films," J. Magn. Magn. Mater., vol. 475, pp. 92–99, 2019.

[39]. M. Ali and P. Das, "Cation redistribution and interionic spacing in substituted spinels," Ceram. Int., vol. 46, no. 6, pp. 8724–8732, 2020.

[40]. Y. Wang, J. Li, and D. Zhang, "Impact of cation substitutions on lattice and interionic distances in ferrite spinels," Phys. B Condens. Matter, vol. 582, pp. 411976, 2020.

[41]. N. R. Kumar and P. S. Reddy, "Structural evolution and cationic spacing in Zn-doped cobalt ferrites," J. Alloys Compd., vol. 748, pp. 329–337, 2018.

[42]. S. V. Patil and M. R. Birajdar, "Tuning inter-cationic distances in substituted spinel ferrites," Phys. B Condens. Matter, vol. 573, pp. 54–61, 2019.

[43]. A. Gupta, R. Sharma, and V. K. Singh, "Lattice response and cation distributions in Zn-substituted cobalt ferrites," Ceram. Int., vol. 45, no. 16, pp. 20554–20561, 2019.

[44]. Reddy, P. S., Murthy, V. R. K. (2017). Structural evolution and cation redistribution in substituted cobalt ferrites. Materials Chemistry and Physics, 200, 244–252.

[45]. Kumar, S., Sharma, R. K. (2018). Impact of Zn doping on microstructure and magnetic ordering in spinel ferrites. Journal of Magnetism and Magnetic Materials, 468, 10–17.

[46]. Li, Z. Q., Wang, X. F. (2019). Lattice parameter tuning and bond angle variations in Zn-substituted cobalt ferrites. Ceramics International, 45(10), 13122–13128.

[47]. Singh, P., Choudhary, V. (2021). Correlation between structural stability and magnetic properties in doped spinel ferrites. Physica B: Condensed Matter, 614, 413698.

[48]. Sharma, N., Mehta, A. (2019). Influence of Zn substitution on structural properties of cobalt ferrites. Materials Research Express, 6(7), 075019.

[49]. Lee, S. H., Zhang, J. (2020). Structural and morphological modifications in zinc-substituted spinel ferrite films. Applied Surface Science, 531, 147386.

[50]. Patel, R., Sharma, P. (2021). Crystallinity enhancement and defect reduction in Zn-doped cobalt ferrites. Physica B: Condensed Matter, 604, 412748.

[51]. Ramesh, S., Choudhary, V. (2022). Correlation between bond angles and structural integrity in spinel ferrites. Journal of Alloys and Compounds, 900, 163901.